^{186}Re-HEDP in the Treatment of Patients with Inoperable Osteosarcoma

Rizwan Syed[1], Jamshed Bomanji[1], Nagesh Nagabhushan[1], Irfan Kayani[1], Ashley Groves[1], Wendy Waddington[1], Anna Cassoni[2], and Peter J. Ell[1]

[1]Institute of Nuclear Medicine, University College Hospital, London, United Kingdom; and [2]Meyerstein Institute of Oncology, University College Hospital, London, United Kingdom

The aim of this study was to examine the safety and efficacy of ^{186}Re-hydroxyethylidene diphosphonate (HEDP) as an adjuvant to external-beam radiotherapy (EBRT) in the treatment of patients with osteosarcoma. **Methods:** Thirteen patients (9 male, 4 female; age range, 12–42 y) were treated with combination chemotherapy (standard U.K. protocol) and ^{186}Re-HEDP therapy (18.5 MBq/kg, intravenously), followed by EBRT. A full blood count; liver function test; and measurements of urea and electrolytes, glomerular filtration rate, and left ventricular function were performed on all patients before and after therapy. Tumor volume and composition were obtained from CT or MRI data. Dosimetric calculations were performed using the MIRD formalism. **Results:** Of the 13 patients, 1 is still under follow-up. The median survival time was 36 mo (range, 12–216 mo) from diagnosis and 5 mo (range, 1–60 mo) from the last ^{186}Re-HEDP treatment. The mean tumor dose delivered with ^{186}Re-HEDP was calculated to be 5.8 Gy (range, 0.5–16 Gy). CT and MRI revealed the tumors to have a complex structure, comprising ''ossified,'' ''partially calcified,'' and ''soft-tissue'' components. Posttherapy scans showed a heterogeneous distribution of ^{186}Re-HEDP in the tumor mass: Although the ''soft-tissue'' component showed minimal uptake of the therapeutic dose, the ''ossified component'' showed intense uptake. The 3 long-term survivors in whom tumor sterilization was achieved received calculated mean tumor doses in the range of 2.0–3.1 Gy, which was believed to be an underestimate of the actual tumor doses delivered. **Conclusion:** This study indicates that a simple approach to tumor dosimetry based on mean tumor dose is inappropriate because it may underestimate the dose delivered to these heterogeneous tumors. The data also indicate that EBRT combined with a standard dose of 18.5 MBq/kg of ^{186}Re-HEDP does not provide a sufficient dose to achieve tumor sterilization. A dose estimation technique is required that is based on the determination of tumor dose at the individual voxel level and that is able to represent the heterogeneous uptake observed in these complex tumor structures with highly nonuniform composition. This, coupled with individualized dose escalation, may then achieve the goal of tumor sterilization.

Key Words: ^{186}Re-HEDP; therapy; inoperable osteosarcoma; external-beam radiotherapy

J Nucl Med 2006; 47:1927–1935

Osteogenic sarcoma is the second most common primary malignant bone tumor, with an incidence of 2.1 cases/million population/y. It is produced by the proliferation of malignant spindle cell stroma directly generating osteoid or immature bone. It most commonly occurs in adolescence, and the most frequent location is around the knee joint (50%). The local recurrence rate is low if treatment is optimal. Overall 5-y survival is 40%–50% (*1,2*).

In the past decade, presurgical chemotherapy has been used with increasing frequency for the management of osteosarcoma. This strategy is responsible for a dramatic increase in survival rates and a marked increase in the percentage of patients treated by limb salvage rather than amputation (*3,4*).

Osteosarcoma is a relatively radioresistant tumor (*5*), and therefore external-beam radiotherapy (EBRT) is used only in the primary treatment of patients with unresectable lesions in the axial skeleton, in palliating metastatic disease, or in patients who refuse definitive surgery (*6*). Tumor sterilization has been reported with high doses (70–80 Gy), but with a significant associated risk of collateral damage (*6*). Targeted tumor therapy using bone-seeking radiopharmaceuticals provides an option to deliver a potentially beneficial adjuvant radiation dose, with little or no collateral damage to the neighboring normal tissue.

Most primary osteosarcomas and their bone metastases show avidity for ^{99m}Tc-hydroxyethylidene diphosphonate (HEDP) (*7*). The ability to bind a β-emitter, ^{186}Re, to HEDP provides a unique opportunity for targeted therapy of these tumors (*8–10*). Here, we present our experience treating 13 osteosarcoma patients with ^{186}Re-HEDP either as an adjunct to high-dose EBRT or as a palliative procedure.

The aim of this study was to assess the degree of toxicity after ^{186}Re-HEDP therapy in pretreated osteosarcoma patients and to calculate the radiation dose delivered by ^{186}Re-HEDP to the tumor mass. An additional aim was to evaluate the safety and efficacy of ^{186}Re-HEDP as an adjuvant to EBRT in these patients.

MATERIALS AND METHODS

Patients

Between March 1999 and December 2004, 13 patients (9 male, 4 female) with histologically proven osteosarcoma and a positive

Received Apr. 7, 2006; revision accepted Sep. 11, 2006.

For correspondence or reprints contact: Jamshed B. Bomanji, MBBS, PhD, Institute of Nuclear Medicine, University College Hospital, 5th Floor, 235 Euston Rd., London NW1 2 BU, U.K.

E-mail: jamshed.bomanji@uclh.nhs.uk

^{99m}Tc-HEDP bone scan result (i.e., showing higher tracer uptake in tumor than in normal bone) were included in the study. The median age of the subjects was 16 y (range, 12–42 y), and their average weight was 52.5 kg (Table 1). All patients consented to receive the therapy. The intent in all patients was palliative.

Of these 13 patients (Table 1), at presentation 5 had primary axial tumors without evidence of metastatic disease. These tumors were inoperable, and ^{186}Re-HEDP therapy was part of the planned initial management strategy to supplement radical external-beam radiation to the primary tumor. All patients had been treated with a standard neoadjuvant chemotherapy protocol, had a clear response after 2 cycles, and had a further response or stable disease after a total of 4 cycles.

One patient who had had an isolated pelvic bone metastasis was treated in the same manner after second-line chemotherapy, receiving a single administration of ^{186}Re-HEDP immediately before 55-Gy EBRT. The remaining patients had established metastatic disease and received ^{186}Re-HEDP after second-line or further chemotherapy with the aim of palliation or maintaining stable disease (Table 2). Eight of these patients had originally been treated with combination chemotherapy followed by surgery of the primary tumor (amputation in 4, limb salvage surgery in 3, or radical radiotherapy in 1). Relapse had occurred at a bony site in only 2 patients and in soft tissue in 6; of the latter, 2 had had previous pulmonary metastasectomies.

All patients underwent a full disease review, a general physical examination, and a routine blood count, liver function tests, glomerular filtration rate test, and measurement of left ventricular ejection fraction before EBRT and radionuclide therapy.

Therapy Protocol

The ^{186}Re-HEDP was purchased from a commercial source (Mallinckrodt Medical Ltd.). Patients were treated as inpatients with an ^{186}Re-HEDP activity of 18.5 MBq/kg. ^{186}Re-HEDP was administered by slow-bolus (approximately 15 s) intravenous injection, with close monitoring of vital signs. Posttherapy scans were obtained at 3–4, 24, 48, and 96 h. Posttherapy response was assessed using the criteria of the World Health Organization (*11*).

Criteria for Rhenium Administration

Inclusion Criteria. Patients with histologic proof of osteosarcoma, radiologically measurable disease, and a ^{99m}Tc-HEDP bone scan positive for lesions were included in this study. All patients gave their informed consent before treatment. Additional requirements included a normal blood count and acceptable renal function (glomerular filtration rate $>$ 50 mL/min/body surface area) at the time of ^{186}Re-HEDP therapy.

Exclusion Criteria. Patients with rapidly progressive soft-tissue disease were excluded from the study. Poor bladder and bowel control were considered relative contraindications.

Dosimetry

Tumor dosimetry was performed using the formalism developed by the MIRD Committee (*12–15*). Adopting the notation of the MIRD schema (*16,17*), the absorbed dose D(t$\leftarrow$s) to target region t from source region s is:

$$D(t \leftarrow s) = \tilde{A}_s \, S(t \leftarrow s), \qquad \text{Eq. 1}$$

where $\tilde{A}_s$ is the cumulated activity (i.e., the total number of nuclear disintegrations) in source region s and S(t$\leftarrow$s) is the source region s–to–target region t S factor (i.e., the mean absorbed dose to target region t per nuclear disintegration in source region s). This formalism permits calculation of the mean absorbed radiation dose delivered to a target region from radioactivity distributed within one or more source regions within the body, and where the source and target may be the same region. In this latter case, it is the "self-irradiation" contribution of the total dose delivered to the target region that is determined, where this is usually the predominant component. In its usual application to diagnostic radiopharmaceuticals, the MIRD schema assumes that the activities and cumulated activities are uniformly distributed within source regions and the radiation energy is uniformly deposited within target regions defined. Thus, if the MIRD formalism is used at the organ level, it is the mean radiation dose within the target organ that is calculated. Use of the MIRD schema has been adapted here to determine the mean absorbed dose delivered to a tumor assumed to be homogeneous in composition, and confined to the component of the total dose that is due to "self-irradiation" by activity distribution within the tumor region itself.

Determination of Tumor Activity from Image Data

Conjugate anterior and posterior whole-body imaging was performed at 0, 4, 24, and typically 96 h after injection using a dual-detector (Maxxus; GE Healthcare) large-field-of-view γ-camera with low-energy high-resolution collimators. The 0-h image dataset was acquired before the patient was allowed to micturate and thus reflected the in vivo retention of all administered activity. Imaging was initially performed at a 15 min/m scan speed, which was modified at later time points to compensate for physical decay of the tracer, and all image counts were adjusted for differences in scan speed.

Irregular regions of interest were defined to encompass the tumor boundaries, generated from the initial image dataset, and overlaid on all subsequent images, correcting for patient placement at each time point. These regions were drawn in direct reference to those placed on the contiguous (transaxial)-slice CT or MRI data, and all possible attempts were made to ensure that these matched as closely as possible. Partial-thickness background correction was also applied using a technique appropriate for a single, well-defined source region surrounded by background activity (*18*) by using representative peripheral irregular background regions of interest and an estimate of fractional tumor thickness if the tumor did not involve the full anteroposterior body thickness at that site. Geometric mean tumor region-of-interest count data were then expressed as the fractional uptake of the geometric mean whole-body counts for the 0-h image dataset—where this is taken to represent 100% of the administered activity in vivo.

Tumor time–activity curves were then plotted from corrected fractional tumor region-of-interest count data, and a single exponential curve was fitted and, if necessary, weighted to the later image time points to better reflect retention of the tracer after the initial phase and physical decay of the tracer. Although this strategy introduces some inaccuracy in the estimation of cumulated tumor activity (represented by the integrated area under the curve), this is a pragmatic strategy in response to the necessity of working with the relatively few image data points gathered for these very sick patients, returning as outpatients after the first 24 h after injection. It is probably reasonable to assume an effectively near-instantaneous uptake of tracer into the osteosarcomatous lesion.

TABLE 1
Patient Profiles and Distribution of Disease

Patient no.	Age at diagnosis (y)	Sex	Weight (kg)	Primary site	Administered activity (MBq)	Tumor absorbed dose (cGy)	Metastases at presentation	History before ^{186}Re-HEDP
1	16	M	50	L tibia	2,820	2.3	No	Ifosfamide; amputation; metastasectomy; lobectomy at 8 y; large bony secondary at 10 y
2	21	F	65	Sacrum	1,410	16 (hip) and 9 (knee)	No	Doxorubicin + cisplatin × 4; progression of primary tumor and lung, bone, and intraabdominal metastases
3	24	M	58.5	Pelvis	5,310	3.1	No	Doxorubicin + cisplatin; progression; etoposide + cisplatin; excision; margin positive; ifosfamide; EBRT: 50 Gy per 11.3 kg (25 fractions) of body weight, paravertebral relapse; HDMTX
4	12	F	40	Ilium	1,350	1.60 and 3.1	No	Cisplatin + ifosfamide (later omitted) + etoposide × 4; HDMTX × 2; good response by primary tumor but pulmonary progression; primary tumor inoperable
5	22	F	61	Distal femur	1,296	2.4	No	Doxorubicin + cisplatin + etoposide; distal femoral replacement; local, nodal, and pulmonary progression at 14 mo
6	42	F	74	Sacrum	1,420	0.5–0.6 (4 sites)	No	Doxorubicin + cisplatin/carboplatin × 6
7	14	M	54	Tibia	1,430	2	No	Doxorubicin + cisplatin × 6; amputation; bone metastasis; HDMTX; ifosfamide; further bone disease
8	12	M	45	Tibia	1,399	2, 2, and 5 (3 sites)	No	Doxorubicin + cisplatin × 6; amputation; pulmonary metastasis at 2 y; metastasectomies; further pulmonary relapse; HDMTX; ifosfamide
9	16	M	44	Distal femur	2,660	1.4 and 2.2	No	Doxorubicin + cisplatin × 6; endoprosthetic replacement; pulmonary, mediastinal, and pleural relapse at 8 mo; ifosfamide + etoposide × 5; partial remission
10	16	M	55.2	Proximal humerus	1,182	14	No	Doxorubicin + cisplatin × 6; disarticulation; adjuvant EBRT to supraclavicular fossa; pulmonary and pleural relapse at 72 mo; metastasectomy and pleurectomy; HDMTX; ifosfamide; etoposide; progressive disease
11	12	M	32	Femur	1,400	1.1 and 2.0	Yes	Doxorubicin + cisplatin × 2; HDMTX; lung progression; endoprosthetic replacement; high-dose ifosfamide (12–14 g/m^2) + etoposide × 3; progressive lung and bone disease
12	16	M	49	Femur	1,430	1.4	No	Doxorubicin + cisplatin × 6, pleural recurrence; resection; ifosfamide + etoposide + MTX; bowel recurrence resected; internal mammary nodes eroding chest wall
13	27	M	55	Ilium + sacrum	1,500	16	No	Doxorubicin + cisplatin + HDMTX; then ifosfamide + etoposide; EBRT to right pelvis; deposit L5 vertebra

HDMTX = high-dose methotrexate.

TABLE 2
Survival After ^{186}Re-HEDP Therapy

Patient no.	Response to treatment	Survival after diagnosis of metastatic disease (mo)	Survival after last ^{186}Re HEDP therapy (mo)	Site of metastases	Subsequent therapy	Follow-up
1	Stable disease: biopsy negative	216	60	Lung	None	Disease-free
2	Stable disease	48	10	Lung	EBRT	Died: perforated bowel
3	Stable disease	36	10	Lung	Ifosfamide; palliative EBRT*	Poor hematologic tolerance of oral etoposide given for palliation; died of gastrointestinal hemorrhage 3 mo after final ^{186}Re-HEDP dose
4	Stable disease	48	1	Lung	Supportive/EBRT	Poor pain control; died at 6 mo
5	Stable disease	12	1	Lung	Supportive†/EBRT	Died at 5 mo: progressive lung disease
6	Stable disease	36	2	Scapula/sternum/thoracic spine	Supportive†/EBRT	Poor pain control: died
7	Lost to follow-up	NA	NA	Lung	EBRT	Lost to follow-up at 3 mo
8	Progressive disease	45	36	Lung/femoral/iliac lymph nodes	Palliative/EBRT	Died at 1 mo of hepatic progression; platelets and white blood cells normal
9	Pain relief at 2 sites but not at third by 1 mo	12	4	Lung/bone	Supportive/EBRT	Died of progressive disease 12 mo after first ^{186}Re-HEDP dose
10	Progressive disease	96	13	Lung	Palliative EBRT 3 mo	Died
11	Progressive disease	36	5	Lung	Palliative EBRT 2 mo	Died at 36 mo
12	No pain relief	20	6	Lung	Supportive/EBRT	Died at 24 mo
13	Progressive disease	30	2	Lung	Palliative EBRT to 1 site at 1 mo	Died

*Profound thrombocytopenia with ifosfamide.
†White blood cells and platelets too low for chemotherapy.

The tumor time–activity data, that is, the non–decay-corrected tumor activity (in MBq), were fit to a monoexponential function:

$$A(t) = a\,e^{-bt}, \quad \text{Eq. 2}$$

where a is the zero-time intercept (in MBq), b the effective clearance constant (in h^{-1}) of the exponential function, and t the time after administration (in h). Integration of this function and normalization to the administered activity yields the tumor cumulated activity per unit administered activity, $\tilde{A}$ (in MBq-h/MBq):

$$\tilde{A} = (a/b)/A_o, \quad \text{Eq. 3}$$

where A_o is the administered activity (in MBq).

Estimation of Mean Tumor Dose

The cumulated activity determined for the tumor above was normalized to the net administered activity (corrected for residual activity within the injection syringe) to obtain the actual cumulated activity for this administration. This figure was then multiplied by the S factor determined below to yield the estimated absorbed dose to the total tumor.

Determination of Tumor Volume, Mass, and S Factor

Contemporaneous or near-contemporaneous CT data were obtained for the tumor site for all but 1 of the patients studied, and with the exception of 2 further patients for whom contemporaneous MRI data of the tumor site were available. Image data were obtained in film format only, necessitating a manual approach to the accurate determination of tumor volume and composition. All image data were reviewed critically, and the boundaries of the tumor were transcribed directly to tracing paper for each contiguous slice. At the same time, this slice was manually segmented into regions determined visually from the underlying CT data as comprising either bone, calcified soft-tissue involvement, "sparsely" calcified soft tissue, or soft tissue, as appropriate; some tumors were deemed to contain only 1 of these components, some 2, and a few all 4. External tumor boundaries were delineated in relation to the limiting functional tumor volume defined by tracer uptake observed from the scintigraphic data.

The total volume represented by each of the 4 tissue components was determined by summation of the traced regions for all slices, using grid-square graph paper as a scaling device. The displayed CT or MR image and knowledge of CT or MRI slice thickness (and pitch data for spiral CT protocols) were then used to normalize this summed area in arbitrary units of "graphical squares" to the true physical size of each tumor region (in cm^3).

Each region was then allocated an appropriate mean tissue density for estimation of its total mass. This was determined as ranging from a tissue density of 1.99 g cm^{-3} for cortical bone to 1.04 g cm^{-3} for soft tissue (taken as skeletal muscle). Tissue regions defined as calcified and sparsely calcified were allocated an intermediate mean density, determined by an assumption of their fractional components by volume. For example, 1 tumor was deemed to have a component of calcified soft tissue best represented, assuming it consisted of 40% cortical bone and 60% soft tissue. Thus, the density in this case was determined to be 1.42 g cm^{-3} (0.4×1.99 g $cm^{-3} + 0.6 \times 1.04$ g cm^{-3}). A further component of sparsely calcified soft tissue was identified to be present within some tumors, where this was likewise assessed by inspection of the CT Hounsfield unit values within the tumor to comprise relative portions assignable to bone and soft tissue reflecting 10% islands of cortical bone within an environment of 90% soft tissue, thus yielding a mean density of 1.14 g cm^{-3} (0.1×1.99 g $cm^{-3} + 0.9 \times 1.04$ g cm^{-3}).

The total mass of each tissue component was then determined from the product of its assigned mean tissue density and the volume estimated from the traced limits defined from the CT data. The total mass of the whole tumor was then calculated.

The appropriate S factor for ^{186}Re for this tumor mass was then determined from the interpolation of a set of S factors for "idealized spheric tumors" accessible through the MIRDOSE3.1 dosimetry software package (*19*). A log–log plot was generated for the $\log_{10}$ S factor for ^{186}Re (in mGy/MBq·s) (*y*-axis) versus the $\log_{10}$ mass of an idealized tumor sphere (in g) (*x*-axis), for which a relationship of $y = -0.9760x - 1.3218$ with a regression of $R^2 = 0.9997$ was obtained. This relationship was then used to determine the S factor for the estimated total tumor mass. The assumption of a spheric geometry does not in itself introduce a significant error, given the relatively short range of the β-particles emitted by ^{186}Re in tissue and their consequent insensitivity to tumor morphology (*20*).

RESULTS

Treatment-Associated Toxicity

Two patients experienced white blood cell and platelet toxicity of more than grade 3 during or after ^{186}Re-HEDP therapy (Table 3). Patient 6 experienced grade 4 platelet toxicity and required a transfusion. For personal reasons, this patient received EBRT to a large pelvic field within 2 mo of ^{186}Re-HEDP therapy, possibly contributing to the marrow toxicity. There were no episodes of neutropenic sepsis. There was, however, evidence of an effect on bone marrow function. In patient 3, administration of palliative oral etoposide, 2 mo after a fourth administration of ^{186}Re-HEDP, produced profound marrow depression, a complication that would not have been expected as a consequence of previous chemotherapy or in the absence of evidence of marrow infiltration by tumor. Poor hematologic tolerance and gastrointestinal bleeding contributed to the death of this patient (Tables 2 and 3).

No significant acute or late bowel toxicity was observed in the 4 patients who underwent EBRT to the pelvis. Although only 1 of these patients has sufficient follow-up for accurate recording of neurologic toxicity, no cauda equina or sacral nerve root toxicity was observed, despite the fact that these structures were within the target volumes of EBRT. There was no deterioration in glomerular filtration rate or left ventricular ejection fraction after EBRT and ^{186}Re-HEDP therapy ($P > 0.05$). In patient 1, who was in chronic renal failure, the glomerular filtration rate was low (46 mL/min) before ^{186}Re-HEDP treatment because of ifosfamide therapy and showed no significant change after treatment.

^{186}Re-HEDP Therapy

The purpose of ^{186}Re-HEDP therapy was to supplement EBRT, to provide palliation to multiple sites, to consolidate the chemotherapy response, and to prolong the duration of

TABLE 3
Treatment-Related Toxicities

Patient no.	Chemotherapy/ ^{186}Re-HEDP interval (mo)	^{186}Re-HEDP/EBRT interval (wk)	Platelet nadir grade	White blood cell nadir grade	WHO status* at ^{186}Re-HEDP therapy	Other toxicity
1	6	3	0	0	1	Preexisting chronic renal failure; no change after ^{186}Re-HEDP therapy
2	6	3	0	0	3	None
3	2	2	2	4	1	Initial toxicity after first course only; white blood cell grade 4 toxicity after 4 cycles; patient recovered but was unable to tolerate palliative chemotherapy
4	2	1.6	3	1	2	Completely resolved at 4 mo
5	8	3	2 on second dose	2	1	None
6	1.5	1	4 during EBRT	3	2	Platelet toxicity persisted at grade 4 for 4 wk and required transfusion; gradually rose but never much beyond 50×10^9/L
7	1.75	2	0	0	1	None
8	36	1	0	0	1	None
9		4	0	0	2	None
10	14	3	0	1	2	None
11	3.5	5	0	1	2	Died within 4 wk because of pulmonary infection (unspecified)
12	5	2	0	0	1	None
13	7	6	0	3	1	None

*Criteria of the World Health Organization (*11*).

stable disease. The single therapeutic activity used for ^{186}Re-HEDP was 18.5 MBq/kg (range, 1,182–5,310 MBq [72−143 mCi]). Of the 13 patients, 10 received a single administration of ^{186}Re-HEDP (1,182–1,500 MBq [32–40.5 mCi]). Two patients received 2 administrations (cumulative activities of 2,660 and 2,820 MBq) of ^{186}Re-HEDP, with a 6-wk interval between them (Table 1). One patient with bone metastases received 4 administrations of ^{186}Re-HEDP (cumulative activity, 5,310 MBq) (Table 1). Mean uptake of ^{186}Re-HEDP by the tumor was 5.8% of the administered activity. No acute side effects were observed after ^{186}Re-HEDP therapy.

Follow-up

Of the 3 patients in whom ^{186}Re-HEDP therapy was used to boost EBRT, 1 is alive with local control 8 y from therapy. The remaining 2 had local progression (Table 2). Of the 11 patients who died, 7 did so because of disease progression, 1 because of intestinal obstruction, and 1 because of intestinal perforation related to intraabdominal disease. Two patients had hemoptysis secondary to lung metastases, and their symptoms abated after EBRT. Seven patients experienced moderate to severe pain, either because of local progression of disease with tumor compression of nerve roots or local expansion of tumor. Overall, partial symptomatic response was observed in 50% and partial tumor response in 30% of patients. One patient received 4 administrations of ^{186}Re-HEDP, and stability was achieved for 12 mo before progression. The remaining patients progressed rapidly after the first ^{186}Re-HEDP therapy and were not considered suitable for further therapy. Of the 13 patients, 1 is still under follow-up and 1 has been lost to follow-up. No patient had complete remission of disease. The median survival time from the diagnosis of metastatic disease was 36 mo (range, 12–216 mo) (Table 2). The median survival time after the last therapeutic dose of ^{186}Re HEDP was 5 mo (range, 1–60 mo) (Table 2). The overall survival rate since the last therapy was 15% at 3 y.

DISCUSSION

In this study, we have presented preliminary data suggestive of the safety of ^{186}Re-HEDP therapy as an adjunct to EBRT in patients with unresectable and metastatic osteosarcoma. To our knowledge, this is the first study to explore the use of EBRT with ^{186}Re-HEDP therapy. In this group of heavily pretreated patients, the adverse effects of ^{186}Re-HEDP therapy were limited to thrombocytopenia and neutropenia and were generally acceptable. However, caution should be exercised in administering second-line chemotherapy to patients who have had several treatments of ^{186}Re-HEDP. It is likely that the bone marrow reserves may have been compromised because of the ^{186}Re-HEDP treatment.

Our study shows that the critical organ for targeted radiotherapy is the bone marrow. ^{186}Re-HEDP uptake in osteosarcomas is a function of regional osteoblastic activity. The marrow within or local to the primary tumor is likely to receive a high absorbed dose, whereas that in nontrabecular normal bone is largely spared. Previous chemotherapy compounds the risk of myelosuppression because the bone marrow reserves are compromised and the marrow may not withstand any further insult. The transient myelosuppression observed in our study supports this assumption, because all patients in our study had received previous chemotherapy. Thus, to circumvent the problems of bone marrow toxicity, stem cell rescue before targeted radionuclide therapy would be required if further dose escalation were to be contemplated.

Clinical data suggest that myelosuppression is less severe after administration of radionuclides with short half-lives (*21*). ^{186}Re-HEDP has a half-life of 3.7 d and decays by emission of β-particles with a mean energy of 1.07 MeV and γ-emission of 137 keV. The latter allows γ-camera imaging of the in vivo distribution of ^{186}Re-HEDP and therefore estimation of tumor and organ absorbed doses. It was for this reason that we chose ^{186}Re-HEDP for therapy.

It has been shown that the targeting ability of ^{186}Re-HEDP depends on the metastatic tumor burden (*22*). In our study, the distribution of ^{186}Re-HEDP within tumors was nonuniform, with the highest amounts of radioactivity deposited where maximum calcification was observed (Fig. 1).

Tumor areas with absent or minimal calcification showed very poor or virtually no uptake of ^{186}Re-HEDP. It can be

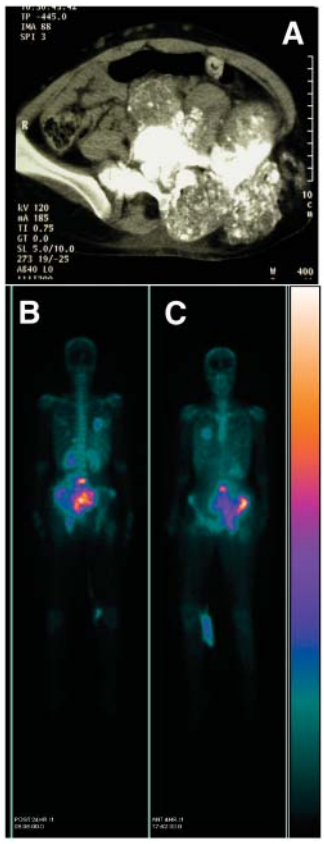

FIGURE 1. In these images of patient 3, CT transaxial slice through tumor site (top) shows massive tumor in left pelvis, and ^{186}Re-HEDP posttherapy whole-body scan (bottom) shows heterogeneous but intense uptake at tumor site in both posterior (left) and anterior (right) views. In addition, metastases are noted in right lung field, L4 vertebra, and left ribs posteriorly.

argued that patients with the osteoblastic-sclerotic subtype would benefit the most from ^{186}Re-HEDP treatment. In this subtype, the tumor cells produce abundant osteoid without large necrotic or fibrotic areas, thus allowing targeting of the tumor mass with greater ^{186}Re-HEDP activity and more uniform dose delivery, without sparing of the isolated pockets of reduced tracer uptake.

It is clear from this study that the mean absorbed tumor dose (0.5–16 Gy) achieved with a conventional ^{186}Re-HEDP dosage of 18.5 MBq/kg is insufficient as an adjunct to EBRT for tumor sterilization. Mean tumor dose was calculated using the MIRD formalism based on the assumption of a uniform distribution of ^{186}Re-HEDP within a homogeneous tumor. However, imaging data from our study showed this assumption not to be valid in osteosarcomas. This is consistent with the findings in our study that 3 long-term survivors in whom tumor sterilization was achieved received doses in the range of 2.0–3.1 Gy, which was believed to be an underestimate of the dose given. It is also known that ^{186}Re-HEDP is taken up and retained by osteoblasts within a 10-μm-thick endosteal layer of normal trabecular and cortical bone (*9*,*23*). Uptake within the disordered osteoblastic region of an osteosarcomatous lesion is usually significantly enhanced, but the reasons for this are not currently understood. Certainly all cell components within this region could be regarded as tissue to be targeted by ^{186}Re-HEDP therapy. The 2 β-particles emitted by ^{186}Re (1.07-MeV β_{max} and 0.93-MeV β_{max}) have a mean range of 0.5 mm in bone and 1 mm in soft tissue, with all β-particles absorbed within 3.4 mm in soft-tissue-equivalent medium. Thus, the cross-fire effect among cells will be significant (*9*,*10*). The mean tumor absorbed dose calculated assuming uniform activity distribution and uniform radiation energy distribution within bone therefore likely does not reflect the biologically effective tumor dose, especially in the significantly disordered tissue architecture characteristic of osteosarcoma, that is, with distinct regions of bone, calcified soft tissue, sparsely calcified soft tissue, or soft tissue. The heterogeneity of the tumor, especially of the osteoid component, and the resulting heterogeneity of activity distribution among different parts of the tumor, as observed by γ-camera imaging, results in a heterogeneous distribution of energy deposition and absorbed dose. This results in absorbed doses to certain portions of the tumor lower than the mean tumor absorbed dose. A more accurate methodology for dosimetry would be required to overcome these limitations of the MIRD-based technique adopted here in support of more aggressive treatment strategies. The MIRD formalism has been extended through the provision of voxel S factors (*24*) to allow nonuniform activity distributions within a region to be addressed at the voxel level. However, these still require that the tissue composition within the region be homogeneous. The Monte Carlo voxel-based approach is an alternative strategy for heterogeneous tissue and one that has been applied in targeted radiotherapy for bone metastases. Samaratunga et al. (*22*) have developed a Monte Carlo simulation model for estimating dose delivery to skeletal metastases after administration of ^{186}Re-HEDP, and the results obtained suggest that a conventional calculation underestimates the dose absorbed by osteoblastic lesions by a factor of 1.8.

CONCLUSION

The standard amount of ^{186}Re-HEDP activity (18.5 MBq/kg) combined with EBRT does not deliver a sufficient adjuvant radiation dose to achieve the target tumor dose of 80 Gy required for sterilization in osteosarcomas. Adverse effects of ^{186}Re-HEDP therapy at the current activity are tolerable and mostly limited to transient myelosuppression. It is assumed that dose escalation of ^{186}Re-HEDP may achieve the objective of tumor sterilization. However, stem cell rescue will be required if myeloablative doses are reached through dose escalation. Finally, tumor dosimetry using the MIRD-based technique used here, which assumes uniform activity distribution of ^{186}Re-HEDP within a homogeneous tumor, is inappropriate and a Monte Carlo voxel-based approach should be used to calculate the dose delivered in these heterogeneously structured tumors. Whether this will be sufficient to overcome the effects of heterogeneous ^{186}Re-HEDP uptake remains to be tested.

REFERENCES

1. Mankin HJ, Hornicek FJ, Rosenberg AE, Harmon DC, Gebhardt MC. Survival data for 648 patients with osteosarcoma treated at one institution. *Clin Orthop.* 2004;429:286–291.
2. Stiller CA, Craft AW, Corazziari I; EUROCARE Working Group. Survival of children with bone sarcoma in Europe since 1978: results from the EUROCARE study. *Eur J Cancer.* 2001;37:760–766.
3. Jaffe N, Patel SR, Benjamin RS. Chemotherapy in osteosarcoma: basis for application and antagonism to implementation; early controversies surrounding its implementation. *Hematol Oncol Clin North Am.* 1995;9:825–840.
4. Taylor WF, Ivins JC, Pritchard DJ, Dahlin DC, Gilchrist GS, Edmonson JH. Trends and variability in survival among patients with osteosarcoma: a 7-year update. *Mayo Clin Proc.* 1985;60:91–104.
5. Gaitan–Yanguas M. A study of the response of osteogenic sarcoma and adjacent normal tissue to radiation. *Int J Radiat Oncol Biol Phys.* 1981;7:593–595.
6. Maxon HR, Thomas SR, Hertberg VS, et al. Re-186 HEDP for the treatment of painful bone metastases. *Semin Nucl Med.* 1992;22:33–40.
7. Maxon HR, Deutsch EA, Thomas SR, et al. Re-186 HEDP for treatment of multiple metastatic foci in bone: human biodistribution and dosimetric studies. *Radiology.* 1988;166:501–507.
8. Englaro EE, Schroder LE, Thomas SR, Williams CC, Maxon HR. Safety and efficacy of repeated sequential administrations of Re-186 HEDP as palliative therapy for painful metastases: initial case reports of two patients. *Clin Nucl Med.* 1992;17:41–44.
9. Spiers FW, Whitwell JR, Beddoe AH. Calculated dose factors for the radiosensitive tissues in bone irradiated by surface-deposited radionuclides. *Phys Med Biol.* 1978;23:481–494.
10. Spiers FW, Beddoe AH, Whitwell JR. Mean skeletal dose factors for beta-particle emitters in human bone. Part II. Surface-seeking radionuclides. *Br J Radiol.* 1981;54:500–504.
11. Miller AB, Hoogstraten B, Staquet M, Winkler A. Reporting results of cancer treatment. *Cancer.* 1981;47:207–214.
12. Loevinger R, Berman M. *A Revised Schema for Calculating the Absorbed Dose from Biologically Distributed Radionuclides. MIRD Pamphlet No. 1, Revised.* New York, NY: Society of Nuclear Medicine; 1976.
13. Howell RW, Wessels BW, Loevinger R, et al. The MIRD perspective 1999. Medical Internal Radiation Dose Committee. *J Nucl Med.* 1999;40(suppl): 3S–10S.
14. Watson EE. Foreword. *J Nucl Med.* 1999;40(suppl):1S–2S.

15. Loevinger R, Budinger T, Watson EE. *MIRD Primer for Absorbed Dose Calculations.* New York, NY: Society of Nuclear Medicine; 1991.
16. Snyder WS, Ford MR, Warner GG, Fisher HL. Estimates of absorbed fractions for monoenergetic photon sources uniformly distributed in various organs of a heterogeneous phantom. MIRD Pamphlet No. 5. *J Nucl Med.* 1969;10(suppl 3):7–14.
17. Snyder WS, Ford MR, Warner GG, Watson SB. *"S": Absorbed Dose per Unit Cumulated Activity for Selected Radionuclides and Organs. MIRD Pamphlet No. 11.* New York, NY: Society of Nuclear Medicine; 1975.
18. Siegel JA, Thomas SR, Stubbs JB, et al. MIRD Pamphlet No. 16: techniques for quantitative radiopharmaceutical biodistribution data acquisition and analysis for use in human radiation dose estimates. *J Nucl Med.* 1999;40(suppl): 37S–61S.
19. Stabin MG. MIRDOSE: personal computer software for internal dose assessment in nuclear medicine. *J Nucl Med.* 1996;37:538–546.
20. de Klerk JM, van Dijk A, van het Schip AD, Zonnenberg BA, van Rijk PP. Pharmacokinetics of rhenium-186 after administration of rhenium-186-HEDP to patients with bone metastases. *J Nucl Med.* 1992;33:646–651.
21. Giannakenas C, Kalofonos HP, Apostolopoulos DJ, Zarakovitis J, Kosmas C, Vassilakos PJ. Preliminary results of the use of Re-186-HEDP for palliation of pain in patients with metastatic bone disease. *Am J Clin Oncol.* 2000;23:83–88.
22. Samaratunga RC, Thomas SR, Hinnefeld JD, et al. A Monte Carlo simulation model for radiation dose to metastatic skeletal tumor from rhenium-186(Sn)-HEDP. *J Nucl Med.* 1995;36:336–350.
23. Whitwell JR, Spiers FW. Calculated beta-ray dose factors for trabecular bone. *Phys Med Biol.* 1976;21:16–38.
24. Bolch WE, Bouchet LG, Robertson JS, et al. MIRD Pamphlet No. 17: the dosimetry of nonuniform activity distributions—radionuclide S values at the voxel level. *J Nucl Med.* 1999;40(suppl):11S–36S.